scientific reports

Check for updates

OPEN

Analysis of the relationships between the degree of migraine with right-to-left shunts and changes in white matter lesions and brain structural volume

Xin Pan[1], Haoran Ren[2], Lili Xie[1], Yu Zou[1], Furong Li[1], Xiaowen Sui[1], Li Cui[1], Zhengping Cheng[1], Jiaojiao Wu[4], Feng Shi[4], Hongling Zhao[1,3]✉ & Shubei Ma[1]✉

To investigate the location of white matter lesions (WMLs) in migraineurs with right–to–left shunts (RLS); the relationships among the severity of WMLs, changes in brain structural volume and RLS shunts; and the relationships among the severity of WMLs, changes in brain structural volume and degree of headache in RLS migraine patients. A total of 102 migraineurs with RLS admitted to the affiliated Central Hospital of Dalian University of Technology from December 2018 to December 2022 were enrolled in this study. RLS flow and the 6-item Headache Impact Test (HIT-6) scores were recorded to reflect the degree of headache. The brain structural volumes of 102 migraineurs with RLS were calculated from T1-weighted images via artificial intelligence, and the brain structural volumes of healthy controls matched according to age and sex were also calculated. The correlations among WML location, RLS, headache degree, WML severity and brain structural volume changes in migraineurs were analyzed. (1) The WMLs of migraineurs with RLS were concentrated mainly in the white matter of the lateral ventricular margin and deep white matter. Subcortical WMLs were concentrated mainly in the parietal lobe, occipital lobe and frontal lobe. (2) There were no significant differences in the WML variables of cerebral white matter high signal volume, ratio of high-signal white matter volume to whole-brain white matter volume (%) or Fazekas score among migraineurs with different RLS flows, but there were significant differences in WML variables among migraineurs with RLS with different HIT-6 grades and MIDAS grades. RLS flow, HIT-6 score and MIDAS grade were not correlated with the WML variables measured in this study. (3) There was a significant difference in the volume of the precentral gyrus between migraineurs with RLS and normal controls ($P < 0.001$), and there was a significant difference between migraineurs with different RLS flows and different HIT-6 scores and peripheral cerebrospinal fluid volumes. There was also a positive correlation between frontal pole structural volume and RLS flow. The volume of the precentral gyrus was negatively correlated with RLS flow, whereas the volume of the pons gyrus was positively correlated with the HIT-6 score. The volume of the temporal pole was negatively correlated with the HIT-6 score. (1) The WMLs of migraineurs with RLS were concentrated mainly in the white matter of the lateral ventricular margin and deep white matter. Subcortical WMLs were concentrated mainly in the parietal lobe, occipital lobe and frontal lobe. (2) There was no correlation between WML severity and RLS flow in migraineurs with RLS. (3) There was no correlation between WML severity and migraine severity in migraineurs with RLS. (4) Volume changes occurred in some brain structures of migraineurs with RLS. (5) Shunt flow and the degree of headache in migraineurs with RLS were correlated with structural volume changes in specific brain regions.

Keywords Migraine, Right-to-left shunt, Degree of headache, White matter lesion, Volume of brain structure

[1]Department of Neurology, Dalian Municipal Central Hospital of Dalian University of Technology, Dalian 116033, Liaoning, China. [2]Department of Neurology, The Third People' s Hospital of Datong Affiliated with Shanxi Medical University, Datong 037046, Shanxi, China. [3]Stroke Center, Dalian Municipal Central Hospital of Dalian University of

Technology, Dalian 116033, Liaoning, China. [4]Department of Research and Development, Shanghai United Imaging Intelligence Co., Ltd., Shanghai 200232, China. ✉email: zhaohongling2000@126.com; mshb1980@vip.163.com

Migraine is a common disease of the nervous system that is characterized by recurrent, unilateral, moderate–to–severe pulsatile headache accompanied by photophobia, phonophobia, nausea, vomiting and other symptoms[1]. In China, it has been reported that migraineurs may experience aura symptoms[2,3]. Previous studies have shown that the annual incidence of migraine in the general adult population is as high as 33 million. The incidence of migraine is greater in women than in men. At the peak age for migraine, the incidence in women is 2–3 times greater than that in men[4–6]. The 2016 Global Burden of Disease (GBD) study revealed that the overall annual prevalence of migraine is 14.4%, with a prevalence of 18.9% for women and 9.8% for men[7]. The pathogenesis of migraine includes sensitization, trigeminal neurovascular system (TVS) damage, calcitonin gene-related peptide (CGRP), and cerebral spreading depression (CSD).

Cardiac right-to-left shunt (RLS) diseases include patent foramen ovale (PFO), ventricular septal defect (VSD), atrial septal defect (ASD), and patent ductus arteriosus (PDA). PFO is the most common RLS disease seen in the clinic, accounting for approximately 95% of all circulatory RLS diseases. RLSs can be classified into three levels: small shunts, medium shunts and large shunts. RLS is closely related to migraine. The incidence of RLS in patients with aura migraine is reportedly 2.5 times greater than that in healthy individuals[8]. The mechanism for this relationship may involve the entrance of a microthrombus into the systemic circulation directly without being filtered by the pulmonary circulation and the inability of hemoglobin to exchange oxygen molecules in the lungs, causing hypoxemia, which affects the cerebrovascular system and trigeminal nervous system, leading to migraine[9]. In addition, RLS can activate platelets and trigger the release of vasoactive substances such as serotonin and CGRP, which aggravate stimulation of the cerebrovascular system and trigeminal nervous system[10]. Finally, the correlation between RLS and migraine may be genetic. One study revealed that some families exhibit autosomal dominant inheritance of RLS associated with aura migraines. Therefore, there may be a specific genetic basis for the abnormality of the atrial septum that is associated with migraine[11].

According to the 2016 GBD study, migraine is the second most common nervous system dysfunction[7] and is associated with anxiety, depression and sleep disorders. Some studies have also shown that migraine may increase the risk of cognitive impairment and cardiovascular and cerebrovascular diseases[12,13]. Migraine attacks often affect the daily activities of patients and seriously affect their work, study and social roles. A questionnaire on the degree of disability related to migraine can be used to quantitatively evaluate the degree of disability caused by migraine. In addition to being used in research, these questionnaires can also help doctors assess the degree of headache in migraineurs. A variety of scales are used to reflect the degree of migraine disability, the most common of which is the 6-item Headache Impact Test (HIT-6). Because the HIT-6 scale is easily understood by the public, it is often used on the internet to help patients understand the burden caused by headaches.

In the context of imaging research, an increasing number of studies have confirmed that migraine with RLS can lead to white matter lesions (WMLs) in migraineurs[14–16]. A study on the relationship between RLS and WMLs by Iwasaki et al.[17] revealed that the presence of RLS is the only independent risk factor for WMLs in migraineurs with RLS. The possible pathogenesis of WMLs in migraineurs with RLS includes abnormal embolism, in which microemboli enter the systemic circulation directly from the venous system, resulting in abnormal embolism and WMLs in migraineurs[18], and vasoactive substances, such as interleukins and serotonin, which directly enter the arterial system due to RLS and stimulate intracranial sensitive neurovascular tissues, resulting in abnormal contraction and relaxation of intracranial blood vessels, headache and WMLs[19]. However, to date, few correlations have been reported between WML severity and RLS flow or headache in migraineurs with RLS. An increasing number of studies have identified functional connectivity changes in the brain regions involved in pain regulation, sensory discrimination, pain cognition and pain emotion in migraineurs through functional magnetic resonance imaging (fMRI), and some brain regions exhibit abnormal activation patterns.

This study focused on migraineurs with RLS to explore where WMLs are more likely to occur, the correlations among RLS flow, WML severity and brain structural volume changes, and the correlations among headache degree, WML severity and brain structural volume changes.

Materials and methods

The subjects of this study were migraineurs with RLS examined at Dalian Central Hospital from December 1, 2018, to December 1, 2022.

Data selection

The inclusion criteria for patients were as follows: (1) headache symptoms were consistent with the International Classification of Headache Disorders, 3rd edition (ICHD-III) proposed by the International Headache Society revised in 2018; (2) a contrast-transcranial Doppler (c-TCD) examination clearly revealed RLS; and (3) a plain MRI scan of the skull, including T1-weighted imaging (T1WI), T2-weighted imaging (T2WI) and fluid-attenuated inversion recovery (FLAIR) sequences, was performed.

The exclusion criteria were as follows: (1) history of cerebrovascular disease; (2) severe intracranial and extracranial macrovascular stenosis and occlusion confirmed by imaging; (3) WMLs with other causes, such as multiple sclerosis; (4) hypertension, diabetes, tumors and other serious medical diseases; and (5) space-occupying lesions observed on head MRI.

Grouping criteria.

To study the correlations among RLS flow, headache degree and WML severity, 102 migraineurs with cardiac RLS were divided into three groups on the basis of RLS flow and four groups on the basis of headache degree. To study the correlations among RLS flow, headache degree and changes in brain structural volume,

102 migraineurs with RLS were included in the study group, and healthy individuals matched by age and sex composed the control group.

We conducted a power analysis to validate our sample size, focusing on whether total frontal pole volume could effectively differentiate between migraineurs and controls. Using G*Power, we determined that a sample size of 102 participants per group was sufficient to achieve near-perfect statistical power with an effect size of 1.87. For the correlation analyses, a minimum of 75 participants was required to ensure adequate power. Increasing the sample size further enhanced statistical power by reducing overlap between groups, thereby improving both specificity and sensitivity, as demonstrated with a sample size of 102 (Supplementary Figs. 1–4).

Research methods

RLS detection methods

A transcranial Doppler (TCD) device was used for c-TCD ultrasonography examination. The main subjects of c-TCD are patients with cryptogenic stroke, migraine, decompression sickness, and other conditions that may be related to a right-to-left shunt (RLS)[20]. The patients were examined in the supine position using a 2-MHz pulsed wave TCD probe with a depth of 50–60 mm, and the unilateral (left or right) middle cerebral artery (MCA) was monitored through the temporal bone window. Ten milliliters of activated normal saline was injected into the median cubital vein of each patient, and the number of high-intensity transient signals (HITS) within 20 s was counted. Saline (10 ml) was reactivated by pellet injection, the patients were instructed to perform the standard Valsalva maneuver, and the number of microemboli within 20 s was counted. HITS were divided into RLS small flows (1–10 HITS), RLS medium flows (11–25 HITS) and RLS large flows (> 25 HITS).

Detection of WMLs and volume changes in 157 brain regions

All of the subjects were scanned with a GE Pioneer 3.0T MR scanner and underwent conventional T1WI, T2WI and FLAIR imaging. The scanning parameters were as follows: repetition time (TR), 1,750 ms; echo time (TE), 24.0 ms; layer thickness, 6 mm; layer number, 20; layer spacing, 1 mm; matrix, 256 × 256; field of view (FOV), 220 mm × 220 mm; and scanning time, 160 s. 2. T2WI parameters: TR, 6,859 ms; TE, 152.2 ms; layer thickness, 6 mm; layer spacing, 1 mm; layer number, 20; matrix, 256 × 256; FOV, 220 mm × 220 mm; and scanning time, 70 s. 3. FLAIR parameters: TR, 12,000 ms; TE, 140 ms; layer thickness, 6 mm; layer spacing, 1 mm; layer number, 20; matrix, 256 × 256; FOV, 220 mm × 220 mm; and scanning time, 160 s.

WMLs exhibited high signal intensity on T2WI and FLAIR images and equal or low signal intensity on T1WI images. To evaluate the severity of WMLs, the intelligent analysis method was applied to high signals in white matter to automatically and synchronously correlate the patients' past examination data and accurately register and compare the lesions. The high-signal volumes of the lateral ventricular margin, periventricular white matter, deep white matter, and subcortical white matter were accurately quantified; the percentage of high-signal cerebral white matter compared with the whole-brain white matter was determined; and the Fazekas score, which effectively indicates ischemic changes, demyelination changes and other pathological processes, was calculated according to authoritative guidelines. Finally, the high-signal report of brain white matter was generated automatically according to the intelligent diagnosis results. The high signal intensity of white matter in the margin of the lateral ventricle was located ≤ 3 mm from the surface of the ventricle; the high signal intensity of periventricular white matter was 3–13 mm away from the surface of the ventricle; the high signal intensity of deep white matter was located between those of the periventricular white matter and subcortical white matter; and the high signal intensity of subcortical white matter was ≤ 4 mm from the cortical medulla junction (Fig. 1).

The whole-brain partition of each patient was based on the T1WI partition and was automatically extracted by a deep learning model trained on the United Imaging platform. Automatic segmentation of the whole brain produced 157 subregions, and the left and right parts of each brain structure were also identified. Once the automatic segmentation results of the deep learning model were obtained, they were evaluated by two senior radiologists with more than 5 years of experience in radiation diagnosis. The intelligent analysis function of brain volume change generated a follow-up curve according to the patient's previous examination results, compared it with the population distribution of big data, and automatically calculated the volume and volume proportions of 157 brain regions (Fig. 2).

Statistical analysis

The data used in this study were analyzed via SPSS 26.0 software, GraphPad and RStudio.

Analysis of WML distribution in migraineurs: The chi-square test was used to compare counting data groups. Continuous variables with a normal distribution are expressed as the mean ± standard deviation and were analyzed via ANOVA. Continuous variables that did not have a normal distribution are expressed as the median (Q1 and Q3), and the Kruskal–Wallis H test was used for analysis. Multiple hypothesis test correction was performed with Dunn's test.

WML difference analysis: Continuous variables with a normal distribution are expressed as the mean ± standard deviation. Continuous variables with a nonnormal distribution are expressed as the median (Q1 and Q3). Categorical variables are expressed as numbers (percentages). The comparison of continuous variables between two groups was performed with a t test for variables that satisfied the criteria of independence, a normal distribution and homogeneity of variance; otherwise, the Mann–Whitney U test was used. For comparisons among three or four groups, an ANOVA was used for variables that satisfied the independence, normal distribution and homogeneity of variance criteria; otherwise, the Kruskal–Wallis H test was used. For comparisons of categorical variables, the chi-square test was used. $P < 0.05$ was considered statistically significant.

Analysis of the differences in brain volume between migraineurs and normal controls: Continuous variables with a normal distribution are expressed as the average ± standard deviation; the independent sample t test was used for analysis, and the difference between the two groups was calculated as the difference in the average.

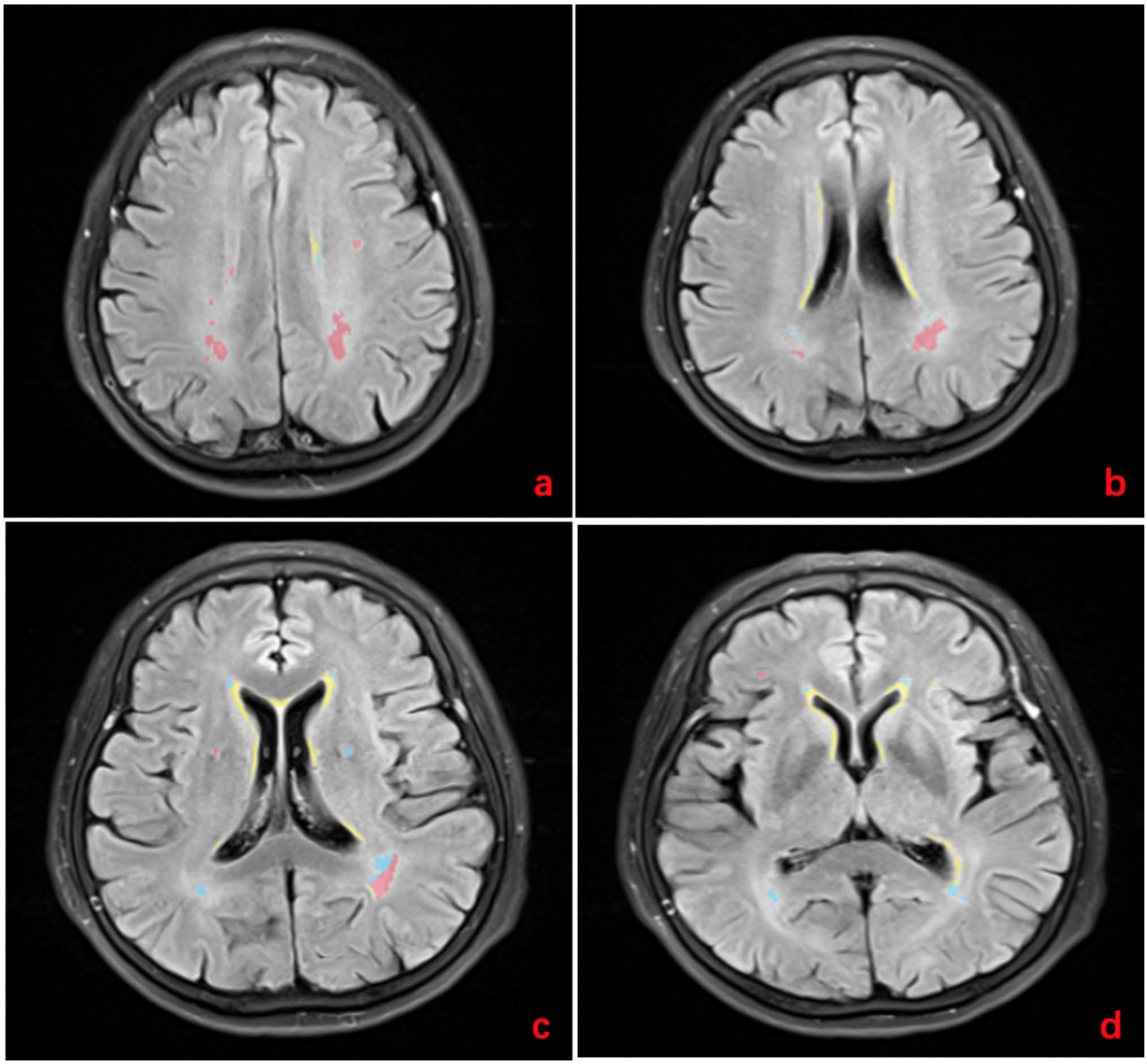

Fig. 1. The intelligent analysis method of high white matter signals was used to accurately quantify the high-signal volume of the lateral ventricular margin, periventricular white matter, deep white matter and subcortical white matter and the proportion of high white matter signals in the whole brain, and the Fazekas score was intelligently calculated according to authoritative guidelines.

Continuous variables that did not have a normal distribution are expressed as the median (Q1–Q3), and the Mann–Whitney U test was used for analysis; the difference between the two groups was calculated as the median difference. Multiple hypothesis tests were corrected by the false discovery rate (FDR). Adjusted $P < 0.001$ indicated statistical significance.

Analysis of the differences among RLS grade, HIT-6 score and changes in brain structural volume: Two-way ANOVA was used for analysis. Multiple hypothesis tests included two-stage Benjamini, Krieger and Yekutieli FDR correction. Adjusted $P < 0.05$ was considered statistically significant.

The correlation between WMLs and brain volume was statistically analyzed via Spearman correlation analysis. The correlation coefficient (r) represents the strength of the correlation: $r \geq 0.90$, very strong correlation; $0.70 \leq r < 0.90$, strong correlation; $0.40 \leq r < 0.70$, moderate correlation; $0.10 \leq r < 0.40$, weak correlation; and $r < 0.10$, negligible correlation. Adjusted $P < 0.001$ was considered statistically significant.

Results

A total of 102 subjects were included in this study, with an average age of 46.9 ± 11.1 years; 33 men (32.4%) and 69 women (67.6%) were included. Among the monthly migraine days, 97 cases (95.1%) experienced fewer than 15 days of migraine (episodic migraine), while 5 cases (4.9%) experienced more than 15 days (chronic migraine).

Fig. 2. Automatic segmentation of the whole brain produced 157 subregions. The volume and volume proportions of these 157 brain regions were calculated accurately, and sagittal, coronal and axial sections of the hippocampus were measured.

Variables	Descriptive statistics
Age (years)	46.9 ± 11.1
Sex, male (n, %)	33 (32.4%)
Female (n, %)	69 (67.6%)
Monthly migraine days (n, %)	
Ÿ < 15 days (episodic migraine)	97 (95.1%)
Ÿ ≥ 15 days (chronic migraine)	5 (4.9%)
The presence of migraine with aura (n, %)	4 (3.9%)
Other comorbidities (n, %)	Anxiety (6, 5.9%), dizziness (7, 6.9%)
Smoking (n, %)	13 (12.7%)
Use of oral contraceptives (n, %)	0 (0.0%)
HIT-6 value (n, %)	
Ÿ ≤ 49 points	3 (2.9%)
Ÿ 50–55 points	13 (12.7%)
Ÿ 56–59 points	23 (22.6%)
Ÿ ≥ 60 points	63 (61.8%)

Table 1. Basic data.

Four subjects presented with migraine with aura. The comorbidities included anxiety (6 patients, 5.9%) and dizziness (7 patients, 6.9%), with no other comorbidities. In the case records, 13 patients smoked, and none of the patients were taking oral contraceptives (Table 1).

Distribution of WMLs in migraineurs with RLS

The WMLs of migraineurs with RLS were mainly concentrated in the white matter of the lateral ventricular margin and deep white matter (Supplementary Table 1). Subcortical WMLs were concentrated mainly in the parietal lobe, frontal lobe and occipital lobe (Fig. 3).

Analysis of the differences in WML variables with different RLS grades

There was no significant difference in any WML variable (volume of high-signal cerebral white matter, percentage of high-signal cerebral white matter volume in the whole-brain white matter volume, or Fazekas score) among migraine patients with different RLS grades.

Analysis of the differences in WML variables across different HIT-6 grades

There were significant differences in the 6 WML variables among migraineurs with RLS with different HIT-6 grades. Notably, no significant results were observed after FDR correction. These 6 variables were right parietal, right temporal, and right cerebellar white matter high signal volume (mm^2) and the corresponding percentages of these regions' white matter in the whole-brain white matter high signal (%) (Table 2). The differential white matter high signals were compared in pairs; the volume and volume proportion of white matter high signals in the same region were consistent (uncorrected $P < 0.05$) (Supplementary Table 2).

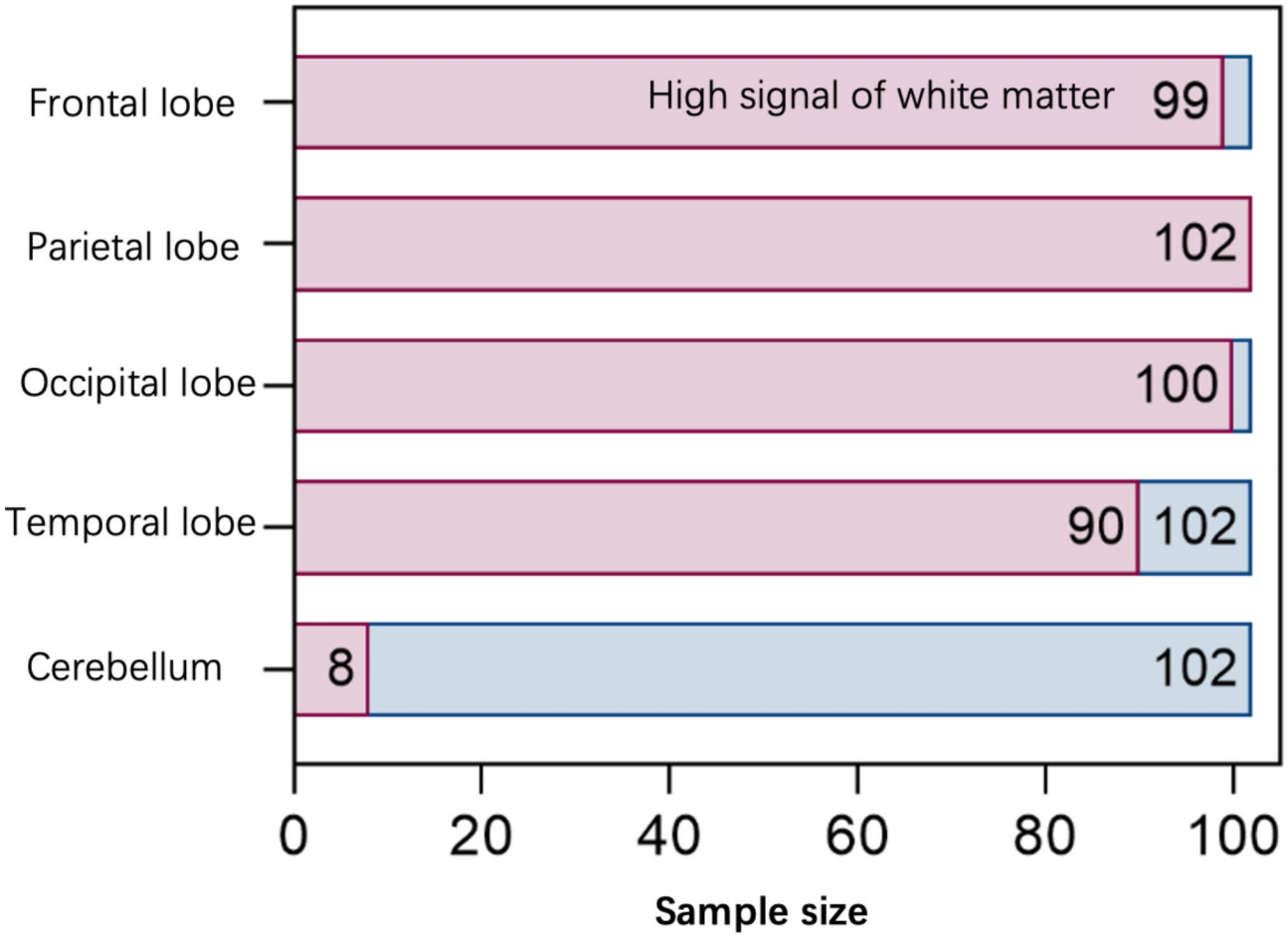

Fig. 3. Comparison of high signal intensity in cortical white matter regions.

Lesion site	Overall ($n=102$)	HIT-6 I ($n=3$)	HIT-6 II ($n=13$)	HIT-6 III ($n=23$)	HIT-6 IV ($n=63$)	*P*
White matter high signal volume (mm^3)						
Right parietal lobe	267.8 (92.3, 852.3)	62.0 (35.4, 81.2)	376.5 (138.5, 862.8)	193.8 (68.9, 351.2)	289.8 (129.2, 1282.7)	0.039
Right temporal lobe	32.8 (0.0, 97.8)	22.4 (0.0, 35.1)	66.7 (0.0, 239.0)	7.4 (0.0, 36.9)	55.4 (1.8, 132.9)	0.023
Right cerebellum	0.0 (0.0, 0.0)	0.0 (0.0, 2.6)	0.0 (0.0, 0.0)	0.0 (0.0, 0.0)	0.0 (0.0, 0.0)	0.017
White matter high signal volume percentage (%)						
Right parietal lobe	5.4 (2.1, 18.8)	1.0 (0.8, 1.6)	7.2 (2.9, 19.9)	4.3 (1.6, 8.5)	5.9 (2.3, 27.4)	0.037
Right temporal lobe	0.7 (0.0, 2.1)	0.4 (0.0, 0.7)	1.4 (0.0, 4.9)	0.2 (0.0, 0.8)	1.1 (0.0, 2.7)	0.027
Right cerebellum	0.0 (0.0, 0.0)	0.0 (0.0, 0.0)	0.0 (0.0, 0.0)	0.0 (0.0, 0.0)	0.0 (0.0, 0.0)	0.017

Table 2. Difference analyses of WML variables across different HIT-6 grades.

Correlation analysis between RLS grades and WML variables

No correlation was found between the RLS grade and the WML variables measured in this study.

Correlation analysis between HIT-6 grades and WML variables

No correlation was found between HIT-6 grades and the WML variables measured in this study.

Brain structure	Overall ($n=102$)	RLS I ($n=24$)	RLS II ($n=30$)	RLS III ($n=48$)	Adjusted P
Total lateral ventricle	14.3 (10.9, 20.6)	17.2 (14.7, 27.1)	19.0 (13.9, 25.5)	19.8 (15.8, 28.5)	< 0.001
Peripheral cerebrospinal fluid	278.3 (251.6, 320.1)	387.2 (356.2, 407.4)	357.7 (339.8, 387.7)	367.7 (346.1, 397.7)	< 0.001
Total cerebellar gray matter	99.2 (92.7, 104.1)	93.3 (88.8, 105.1)	94.4 (88.7, 97.6)	91.7 (87.4, 97.9)	< 0.001
Left cerebral white matter	216.8 ± 22.04	181.1 ± 22.39	186.6 ± 24.07	184.0 ± 18.80	< 0.001
Right cerebral white matter	217.0 ± 22.03	181.2 ± 24.10	185.9 ± 23.40	185.0 ± 18.93	< 0.001
Total cerebral white matter	433.8 ± 44.0	362.3 ± 46.2	372.5 ± 47.3	369.0 ± 37.5	< 0.001

Table 3. Differential analysis of brain structural volume across different RLS grades.

Brain structure	HIT-6 0 ($n=102$)	HIT-6 I ($n=3$)	HIT-6 II ($n=13$)	HIT-6 III ($n=23$)	HIT-6 IV ($n=63$)	Adjusted P
Total lateral ventricle	14.3 (10.9, 20.6)	20.2 (5.5, 26.2)	16.9 (14.7, 26.1)	17.5 (11.3, 30.2)	19.6 (15.4, 29.1)	< 0.001
Total cerebral white matter	433.8 ± 44.0	399.7 ± 45.0	371.6 ± 42.8	359.6 ± 40.1	369.5 ± 43.1	< 0.001
Total cerebellar white matter	25.2 (23.7, 26.6)	21.0 (17.9, 21.0)	19.8 (17.8, 21.7)	20.0 (17.5, 20.7)	19.0 (17.5, 21.0)	< 0.001
Left cerebral white matter	216.8 ± 22.04	198.0 ± 21.12	185.1 ± 21.43	179.5 ± 20.61	184.8 ± 21.44	< 0.001
Right cerebral white matter	217.0 ± 22.03	201.7 ± 23.89	186.5 ± 21.50	180.1 ± 19.58	184.7 ± 21.96	< 0.001
Peripheral cerebrospinal fluid	278.3 (251.6, 320.1)	386.7 (279.2, 396.5)	375.1 (347.0, 410.2)	364.2 (342.3, 386.8)	369.5 (344.5, 398.3)	< 0.001

Table 4. Differential analysis of brain structural volume across different HIT-6 grades.

Analysis of the difference in brain structural volume between migraineurs and normal controls

The differences in brain structural volume between migraineurs and normal controls were analyzed. After FDR correction, a total of 42 brain subregions were higher and 58 brain subregions were lower in migraine patients than in normal controls (*adjusted* $P < 0.001$), as shown in Supplementary Tables 3~4, respectively. Detailed descriptions are given in the Supplementary Results.

Analysis of the differences in brain structural volume changes across different RLS grades

There were statistically significant differences in total lateral ventricle volume, right cerebral white matter volume, left cerebral white matter volume, total cerebellar gray matter volume and peripheral cerebrospinal fluid volume between different RLS grades, with *FDR-adjusted* $P < 0.001$ (Table 3). In the pairwise comparisons of these differential brain structures, the statistical results were consistent (Supplementary Table 5).

Analysis of the differences in brain structural volume changes across different HIT-6 grades

There were statistically significant differences in total lateral ventricle volume, total cerebral white matter volume, total cerebellar white matter volume, left cerebral white matter volume, right cerebral white matter volume and peripheral cerebrospinal fluid volume among different HIT-6 grades, with *FDR-adjusted* $P < 0.001$ (Table 4). In the pairwise comparisons of these differential brain structures, the statistical results were consistent (Supplementary Table 6).

Analysis of the correlation between RLS flow and brain structural volume

As shown in Table 5, five strong correlations ($r \geq 0.70$) were observed between RLS flow and brain structural volume (*FDR-adjusted* $P < 0.001$). Specifically, the volumes of the frontal lobe (left frontal pole) and subcortical gray matter structures (ventral diencephalon) were positively correlated with RLS flow, and the volume of the fourth ventricle was negatively correlated with RLS flow. In addition, multiple moderate correlations ($0.40 \leq r < 0.70$) are summarized in Supplementary Table 7.

The volumes of the frontal lobe (total frontal pole and orbital part), temporal lobe (superior temporal gyrus), optic chiasm, pons, corpus callosum, lateral ventricle, third ventricle and peripheral cerebrospinal fluid were moderately positively correlated with RLS flow. The volumes of the caudal part of the middle frontal gyrus, precentral gyrus), temporal lobe (slope part of the superior temporal gyrus, temporal pole, fusiform gyrus, entorhinal cortex, and parahippocampal gyrus), paracentral lobule, occipital lobe (rectangular gyrus), subcortical gray matter structures (globus pallidus), cerebellar gray matter, and cerebral white matter were moderately negatively correlated with RLS flow.

Brain structures	Correlation coefficient	95% confidence interval (CI)	Adjusted *P*
Strong correlations ($r \geq 0.70$)			
Total ventral diencephalon	0.758	[0.693, 0.811]	< 0.001
Right ventral diencephalon	0.750	[0.683, 0.804]	< 0.001
Left ventral diencephalon	0.744	[0.676, 0.800]	< 0.001
Left frontal pole	0.719	[0.645, 0.779]	< 0.001
Fourth ventricle	− 0.700	[− 0.764, − 0.622]	< 0.001

Table 5. Correlation analysis between RLS flow and brain structural volume. The strong correlations are listed below.

Brain structure	Correlation coefficient	95% CI	Adjusted *P*
Strong correlations ($r \geq 0.70$)			
Total ventral diencephalon	0.803	[0.748, 0.847]	< 0.001
Right ventral diencephalon	0.802	[0.747, 0.846]	< 0.001
Left ventral diencephalon	0.781	[0.721, 0.830]	< 0.001
Left frontal pole	0.769	[0.706, 0.820]	< 0.001
Optic chiasm	0.761	[0.697, 0.814]	< 0.001
Middle part of corpus callosum	0.742	[0.673, 0.798]	< 0.001
Left cerebellar white matter	− 0.746	[− 0.802, − 0.679]	< 0.001
Fourth ventricle	− 0.740	[− 0.797, − 0.671]	< 0.001
Total cerebellar white matter	− 0.710	[− 0.772, − 0.635]	< 0.001

Table 6. Correlation analysis between HIT-6 grades and brain structural volume. The strong correlations are listed below.

Analysis of the correlation between HIT-6 grades and brain structural volume changes

As shown in Table 6, nine strong correlations ($r \geq 0.70$) were observed between HIT-6 grades and brain structural volume (*FDR-adjusted* $P < 0.001$). Specifically, the volumes of the frontal lobe (left frontal pole), subcortical gray matter structures (ventral diencephalon), optic chiasm, and corpus callosum were positively correlated with the HIT-6 grade, and the volumes of the cerebellar white matter and fourth ventricle were negatively correlated with the HIT-6 grade. In addition, multiple moderate correlations ($0.40 \leq r < 0.70$) are summarized in Supplementary Table 8. The volumes of the frontal lobe (frontal pole and orbital part), temporal lobe (superior temporal gyrus), third ventricle, pons, lateral ventricle, and peripheral cerebrospinal fluid were moderately positively correlated with the HIT-6 grade. The volumes of the frontal lobe (precentral gyrus, caudal part of the middle frontal gyrus), paracentral lobule, temporal lobe (parahippocampal gyrus, temporal pole, slope part of the superior temporal gyrus, fusiform gyrus), occipital lobe (rectangular gyrus), and subcortical gray matter structures (globus pallidus, nucleus accumbens) were moderately negatively correlated with HIT-6 grades.

Analysis and discussion

In this study, the WMLs of migraineurs with RLS were found to be concentrated mainly in the lateral ventricular marginal white matter and deep white matter. A retrospective study of 425 headache patients (303 women; 242 migraineurs, 183 tension-type headache patients) revealed an increased prevalence of deep WMLs in migraineurs with RLS[14]. Mark C. Kruit et al.[21] reported that the incidence of deep WMLs in female migraineurs was greater than that in control individuals and that deep WMLs increased with increasing migraine attack frequency but were not related to migraine subtype; in addition, there was no correlation between periventricular WML severity and sex, migraine frequency or migraine subtype in migraineurs. At present, there are few studies on the distribution of WMLs in the lateral ventricular marginal white matter and deep white matter in migraineurs with RLS, and more studies are needed to determine the pathogenesis.

In addition, we found that subcortical WMLs were concentrated in the parietal frontal lobe and occipital lobe in migraineurs with RLS. A study by Signorielloe et al.[22] revealed that PFO may be associated with WMLs in migraineurs and that WMLs are more likely to occur in the occipital lobe; in particular, visual aura was associated with occipital lobe lesions. Another study showed that in migraineurs[23], RLS was associated with near-cortical WMLs, mainly in the frontal and parietal lobes, which are located in the blood supply area of the anterior cerebral artery. However, the exact mechanism underlying this effect is not clear. The WMLs near the cortex may be caused by the mechanism of embolization. With changes in chest pressure, microemboli intermittently enter the brain due to RLS in the heart. This mechanism may occur because the anterior cerebral artery is the direct continuation of the end of the internal carotid artery, and the blood flow resistance is lower than that in other large intracranial arteries; thus, the microemboli can easily enter the distribution area of the anterior cerebral artery and then distribute along the blood vessels to the farthest end. However, a limitation of

this study is that migraineurs without RLS were not included in the control group, preventing a better reflection of the WML distribution characteristics of migraine patients with RLS.

With respect to the relationship between WML severity and RLS flow in migraineurs with RLS, a multicenter study in 2018 involving 334 migraineurs[23,24] reported that WML severity in migraineurs with RLS was not associated with RLS flow. The conclusions of this study are consistent with those of previous studies. Similarly, another study revealed that WMLs do not increase with increasing RLS flow[24,25]. Park et al.[14] reported a correlation between RLS flow and deep WMLs (OR = 3.240, $P < 0.01$), and RLS was an independent risk factor for the severity of small deep WMLs. The varying conclusions of these studies may be related to differences in the race of the participants, the definition and classification of WMLs, age, MRI equipment, setting parameters and research methods.

This study revealed no relationship between WML severity and headache severity in migraineurs with RLS. A study by Junyan Huo et al.[23,27] suggested that the severity of WMLs in migraineurs with RLS was not related to the severity or duration of headache. This finding is consistent with the results of previous studies[23,25–32].

Currently, some neuroscientists believe that the pathophysiology of migraine has evolved from the initial vasodilation hypothesis to brain dysfunction involving pain and other organ processing[33]. Neuroscientists have used fMRI to observe the brain under visual, olfactory, cognitive, motor and other stimuli, which can induce migraine attacks, increasing the understanding of the pathogenesis of migraine. Under pain stimulation, abnormal activation has been observed in the brain regions involved in pain regulation, sensory discrimination, pain cognition and pain emotion. The activation of the thalamus, hippocampus, temporal pole, middle cingulate gyrus and fusiform gyrus increased, and the activation of brain regions such as the secondary somatosensory cortex and precentral gyrus decreased. Under olfactory stimulation, cortical structures related to smell, such as the temporal pole and superior temporal gyrus, are abnormally activated[34]. In addition, the rostral structure of the pontine, which is closely related to the trigeminal pain pathway, is abnormally activated, which explains the symptoms of osmophobia in migraineurs and why a specific smell can induce migraine attacks. Under visual stimulation, the visual cortex is significantly activated[35,36], which may explain photophobia during migraine attacks and why visual stimulation can induce headache attacks. Abnormalities in brain networks and functional connections, including the occipital lobe, sensorimotor network, bilateral lateral and inferior cerebellum, cingulate network, default mode network and frontoparietal network, can also be observed in migraineurs at rest[37,38]. In recent years, studies on the brain networks of migraineurs and models of dynamic functional connectors have shown that the thalamus, occipital lobe and basal nucleus play important roles in transmitting pain, regulating vision and integrating pain[39,40].

An increasing number of studies have revealed evidence of structural abnormalities in gray matter in migraineurs, suggesting that gray matter is related to the neural network involved in pain management. In some studies, surface-based morphology (SBM) and voxel-based morphology (VBM) were used, and a significant decrease was observed in gray matter volume in some regions, such as the left precentral gyrus, right superior temporal gyrus and right inferior frontal gyrus, which participate in the pain loop[41], and the volume of gray matter in visual areas V3 and V5 of the right occipital cortex decreased[42]. The volume of the spinal trigeminal nucleus, which is involved in the transmission and regulation of intracranial vascular and meningeal trauma information, and the cerebellum, which is involved in pain information, decreases[43]. However, other studies have shown that the thicknesses of certain areas of the cortex can also be increased in migraineurs[44–46].

Diffusion tensor imaging (DTI) can reveal the structure of white matter, especially the course and structure of the axons of nerve cells. Planchuelo-Gómez et al.[47] reported a positive correlation between the course of chronic migraine and bilateral external fractional anisotropy (FA) and a negative correlation between the onset time of chronic migraine and the average radial diffusivity (RD) value of the bilateral external capsule. These findings indicate that there are differences in white matter structure between paroxysmal migraine and chronic migraine. Compared with that of patients with paroxysmal migraine, the axonal integrity of patients with chronic migraine is impaired in the early stage of headache attack. Porcaro et al.[48] analyzed the DTI parameters of the whole hypothalamus and its subregions in 20 patients with aura migraine during headache attack and 20 healthy controls. Compared with those in the healthy control group, the mean diffusivity (MD), axial diffusivity (AD) and RD in the hypothalamus of patients with aura migraine changed significantly. These findings indicate that the hypothalamus plays an important role in the pathogenesis of aura migraines.

In summary, migraine can affect the white matter and gray matter of the human brain, but studies on the volume changes in these 157 brain regions in migraineurs with RLS are lacking. In this study, the brain structural volume of migraineurs with RLS changed significantly in the paracentral lobule, precentral gyrus, postcentral gyrus, inferior parietal lobule, supramarginal gyrus, anterior cuneiform lobe, temporal pole, superior temporal gyrus, inferior temporal gyrus, lateral occipital gyrus, fusiform gyrus, rectangular gyrus, superior frontal gyrus, middle frontal gyrus, frontal pole, medial orbitofrontal lobe, lateral orbitofrontal lobe, orbital part, lingual gyrus, cingulate gyrus, entorhinal cortex, parahippocampal gyrus, optic chiasm, globus pallidus, caudate nucleus, nucleus accumbens, putamen, ventral diencephalon, pons, cerebellar gray matter, choroid plexus, corpus callosum, cerebral white matter, cerebellar white matter, lateral ventricle, third ventricle, fourth ventricle, and peripheral cerebrospinal fluid. The volumes of the frontal pole, temporal pole, slope part of the superior temporal gyrus, fusiform gyrus, rectangular gyrus, anterior cuneiform lobe, lateral occipital gyrus, supramarginal gyrus, lingual gyrus, optic chiasm, pons, ventral diencephalon, corpus callosum, third ventricle, peripheral cerebrospinal fluid, entorhinal cortex, cingulate gyrus, parahippocampal gyrus, globus pallidus and nucleus accumbens were also significantly correlated with RLS flow and headache severity. These findings indicate that the human brain exhibits adaptive changes in response to migraine. However, the mechanism underlying this phenomenon is not clear. Previous studies have shown that some symptoms of migraine can be caused by the excitation of dopaminergic neurons and that migraineurs are highly sensitive to dopamine receptors[49–51]. Dopamine receptors are distributed in the caudate nucleus, putamen, amygdala, nucleus accumbens, lateral

papillary nucleus, Calleja island, hypothalamus, hippocampus, medial temporal lobe, optic tract, cerebral cortex, telencephalon, frontal cortex, and retina, among others. This finding is highly consistent with the changes in brain volume observed in this study, which may indicate that some changes in brain structural volume in this study may be related to the involvement of dopamine in the pathogenesis of migraine.

An in-depth study of the factors related to brain structural volume changes in migraineurs with RLS may provide clues for exploring the pathogenesis of migraine with RLS. This study is novel in that, to date, no correlation study on the changes in brain structural volume in migraineurs with RLS has been performed. However, the sample size included in this study was small and therefore prone to bias errors. In addition, the changes in brain structural volume in migraineurs without RLS were not compared with those in migraineurs with RLS to determine the specificity of brain structural volume changes.

Migraine is a complex disease that can be affected by different psychological conditions, different environments, and biochemical and neurophysiological factors[36]. The threshold of headache differs depending on the individual. Even in the same patient, the threshold of headache will change under different conditions. Moreover, headache can be caused by a variety of factors or one decisive factor, such as fluctuations in estrogen, which plays a decisive role in menstrual migraine[52]. All of the above factors may have had an impact on the results of the study.

The main limitations of this study are as follows: (1) With respect to imaging methods, the thickness and spacing of head MR images are relatively large, which results in some lesions being missed, which impacts the results of the study. (2) In this study, migraineurs without RLS were not included in the control group to reflect the specificity of WMLs and brain structural volume changes in migraineurs with RLS. (3) The small sample size is the main limitation of this study. The sample size is small because this study was a single-center study, and strict inclusion and exclusion criteria were implemented to determine the number of subjects. All migraineurs with RLS had to meet the international diagnostic criteria for headache classification, and drug abuse and other types of headache had to be excluded, slowing the case inclusion speed. Subsequent collection of cases will continue to expand the sample size and allow further analysis.

Our understanding of the relationships among migraine with RLS, WMLs and brain structural volume changes is constantly developing, and many studies on related mechanisms and manifestations on neuroimaging, including structural and functional imaging, are ongoing. The changes in brain structure and function in migraineurs vary. Therefore, it is important to explore whether migraineurs with RLS have specific bioimaging changes, the causal relationship between imaging changes and migraine, and whether occlusion of the PFO can affect the brain structure or function of migraineurs to improve migraine symptoms. Therefore, it will be necessary to use multimode magnetic resonance technology to perform larger sample, multicenter and prospective studies in the future.

Conclusion

(1) The WMLs of migraineurs with RLS were concentrated mainly in the white matter of the lateral ventricular margin and deep white matter. Subcortical WMLs were concentrated mainly in the parietal lobe, occipital lobe and frontal lobe. (2) There was no correlation between WML severity and RLS flow in migraineurs with RLS. (3) There was no correlation between the severity of WMLs and the degree of migraine in migraineurs with RLS. (4) Volume changes were found in the brain structure of migraineurs with RLS. (5) The RLS flow and degree of headache in migraineurs with RLS were correlated with structural volume changes in some brain regions.

Data availability

The datasets used and analysed during the current study are available from the corresponding author (mshb1980@vip.163.com) on reasonable request.

Received: 27 July 2024; Accepted: 1 January 2025
Published online: 07 January 2025

References

1. Ran, Y. et al. Gradually shifting clinical phenomics in migraine spectrum: a cross-sectional, multicenter study of 5438 patients. *J. Headache Pain*. **23**(1), 1–14 (2022).
2. Dong, Z. et al. Application of ICHD-II criteria in a headache clinic of China. *PloS One*. **7**, e50898 (2012).
3. Wang, S. J. et al. Prevalence of migraine in Taipei, Taiwan: a population-based survey. *Cephalalgia: Int. J. Headache*. **20**(6), 566–572 (2000).
4. Khil, L. et al. Incidence of migraine and tension-type headache in three different populations at risk within the German DMKG headache study. *Cephalalgia: Int. J. Headache*. **32**(4), 328–336 (2012).
5. Lyngberg, A. C. et al. Incidence of primary headache: a Danish epidemiologic follow-up study. *Am. J. Epidemiol.* **161**(11), 1066–1073 (2005).
6. Baykan, B. et al. Migraine incidence in 5 years: a population-based prospective longitudinal study in Turkey. *J. Headache Pain*. **16**, 103 (2015).
7. GBD 2016 Headache Collaborators. Global, regional, and national burden of migraine and tension-type headache, 1990–2016: a systematic analysis for the global burden of Disease Study 2016. *Lancet Neurol.* **17**(11), 954–976 (2018).
8. Schwerzmann, M. et al. Prevalence and size of directly detected patent foramen ovale in migraine with aura. *Neurology* **65**(9), 1415–1418 (2005).
9. Hildick-Smith, D. & Williams, T. M. Patent foramen ovale and migraine headache. *Interventional Cardiol. Clin.* **6**(4), 539–545 (2017).
10. Demir, B. et al. Mean platelet volume is elevated in patients with patent foramen ovale. *Archives Med. Science: AMS*. **9**(6), 1055–1061 (2013).
11. Wilmshurst, P. T. et al. Inheritance of persistent foramen ovale and atrial septal defects and the relation to familial migraine with aura. *Heart* **90**(11), 1315–1320 (2004).

12. Huang, L. et al. Duration and frequency of migraines affect cognitive function: evidence from neuropsychological tests and event-related potentials. *J. Headache Pain*. **18**(1), 54 (2017).
13. Goadsby, P. J., Lipton, R. B. & Ferrari, M. D. Migraine–current understanding and treatment. *N. Engl. J. Med.* **346**(4), 257–270 (2002).
14. Park, H-K. et al. Small deep white matter lesions are associated with right-to-left shunts in migraineurs. *J. Neurol.* **258**(3), 427–433 (2011).
15. Yoon, G-J. et al. Right-to-left shunts as a cause of juxtacortical spots in patients with migraine. *Eur. J. Neurol.* **19**(8), 1086–1092 (2012).
16. Kim, B. J. et al. Imaging characteristics of ischemic strokes related to patent foramen ovale. *Stroke Am. Heart Association*. **44**(12), 3350–3356 (2013).
17. Haller, S. et al. Do brain T2/FLAIR white matter hyperintensities correspond to myelin loss in normal aging? A radiologic-neuropathologic correlation study. *Acta Neuropathol. Commun.* **1**, 14 (2013).
18. De Benedittis, G. et al. Magnetic resonance imaging in migraine and tension-type headache. *Headache* **35**(5), 264–268 (1995).
19. Afridi, S. K. et al. A positron emission tomographic study in spontaneous migraine. *Arch. Neurol.* **62**(8), 1270–1275 (2005).
20. Xing, Y. & Lin, P. *Clinical Manual for Contrast-enhanced Transcranial Doppler* (Science and technology of China, 2022).
21. Kruit, M. C. et al. Migraine as a risk factor for subclinical brain lesions. *JAMA* **291**(4), 427–434 (2004).
22. Signoriello, E. et al. Migraine as possible red flag of PFO presence in suspected demyelinating disease. *J. Neurol. Sci.* **390**, 222–226 (2018).
23. Huo, J. et al. Small demyelination of the cortex may be a potential marker for the right-to-left shunt of the Heart. *Brain Sci.* **12**(7), 884 (2022).
24. Jiang, X-H. et al. Right-to-left shunt and subclinical ischemic brain lesions in Chinese migraineurs: a multicentre MRI study. *BMC Neurol.* **18**(1), 18 (2018).
25. Uggetti, C. et al. Migraine with aura and white matter lesions: an MRI study. *Neurol. Sci.* **38**, 11–13 (2017).
26. Toghae, M. et al. The prevalence of magnetic resonance imaging hyperintensity in migraine patients and its association with migraine headache characteristics and cardiovascular risk factors. *Oman Med. J.* **30**(3), 203–207 (2015).
27. Kruit, M. C. et al. Migraine is associated with an increased risk of deep white matter lesions, subclinical posterior circulation infarcts and brain iron accumulation: the population-based MRI CAMERA study. *Cephalalgia: Int. J. Headache*. **30**(2), 129–136 (2010).
28. Swartz, R. H. & Kern, R. Z. Migraine is associated with magnetic resonance imaging white matter abnormalities: a meta-analysis. *Arch. Neurol.* **61**(9), 1366–1368 (2004).
29. Trauninger, A. et al. Risk factors of migraine-related brain white matter hyperintensities: an investigation of 186 patients. *J. Headache Pain*. **12**(1), 97–103 (2011).
30. Gaist, D. et al. Migraine with aura and risk of silent brain infarcts and white matter hyperintensities: an MRI study. *Brain: J. Neurol.* **139**(Pt 7), 2015–2023 (2016).
31. Santamarta, E. et al. Chronic migraine does not increase posterior circulation territory (PCT) infarct-like lesions. *J. Neurol. Sci.* **336**(1), 180–183 (2014).
32. Meilán, A. et al. No association between migraine frequency, white matter lesions and silent brain infarctions: a study in a series of women with chronic migraine. *Eur. J. Neurol.* **27**(8), 1689–1696 (2020).
33. Goadsby, P. J. et al. Pathophysiology of migraine: a disorder of sensory processing. *Physiol. Rev.* **97**(2), 553–622 (2017).
34. Stankewitz, A. & May, A. Increased limbic and brainstem activity during migraine attacks following olfactory stimulation. *Neurology* **77**(5), 476–482 (2011).
35. Griebe, M. et al. Multimodal assessment of optokinetic visual stimulation response in migraine with aura. *Headache: J. Head Face Pain*. **54**(1), 131–141 (2014).
36. Huang, J. et al. fMRI evidence that precision ophthalmic tints reduce cortical hyperactivation in migraine. *Cephalalgia* **31**(8), 925–936 (2011).
37. Cui, W. et al. MRI evaluation of the relationship between abnormalities in vision-related brain networks and quality of life in patients with migraine without aura. *Neuropsychiatr. Dis. Treat.* **17**, 3569–3579 (2021).
38. Tu, Y. et al. An fMRI-based neural marker for migraine without aura. *Neurology* **94**(7), e741–e751 (2020).
39. Chen, D. et al. Brain functional connectivity in patients with migraine based on complex networks analysis. *Chin. J. Med. Imaging*, 418–422. (2015).
40. Nie, W. et al. Extraction and analysis of dynamic functional connectome patterns in migraine sufferers: a resting-state fMRI study. *Comput. Math. Methods Med.* **2021**, 6614520 (2021).
41. Valfrè, W. et al. Voxel-based morphometry reveals gray matter abnormalities in migraine. *Headache: J. Head Face Pain*. **48**(1), 109–117 (2008).
42. Palm-Meinders, I. H. et al. Volumetric brain changes in migraineurs from the general population. *Neurology* **89**(20), 2066–2074 (2017).
43. Z, Q. & Xw, H. J Z, et al. Structural changes of cerebellum and brainstem in migraine without aura. The journal of headache and pain. *J. Headache Pain*, **20**(1). (2019).
44. Zhang, J. et al. Assessment of gray and white matter structural alterations in migraineurs without aura. *J. Headache Pain*. **18**(1), 74 (2017).
45. Kim, J. H. et al. Thickening of the somatosensory cortex in migraine without aura. *Cephalalgia: Int. J. Headache*. **34**(14), 1125–1133 (2014).
46. Granziera, C. et al. Anatomical alterations of the visual motion processing network in migraine with and without aura. *PLoS Med.* **3**(10), e402 (2006).
47. Planchuelo-Gómez, Á. et al. White matter changes in chronic and episodic migraine: a diffusion tensor imaging study. *J. Headache Pain*. **21**(1), 1 (2020).
48. Porcaro, C. et al. Hypothalamic structural integrity and temporal complexity of cortical information processing at rest in migraine without aura patients between attacks. *Sci. Rep.* **11**(1), 18701 (2021).
49. Barbanti, P. et al. Dopaminergic symptoms in migraine. *Neurol. Sci.* **34**, 67–70 (2013).
50. de Sousa, S. C. et al. A dopamine D4 receptor exon 3 VNTR allele protecting against migraine without aura. *Annals Neurology: Official J. Am. Neurol. Association Child. Neurol. Soc.* **61**(6), 574–578 (2007).
51. Barbanti, P. et al. Migraine patients show an increased density of dopamine D3 and D4 receptors on lymphocytes. *Cephalalgia: Int. J. Headache*. **20**(1), 15–19 (2000).
52. Welch, K. M. A. Contemporary concepts of migraine pathogenesis. *Neurology* **61**(8 Suppl 4), S2–8 (2003).

Acknowledgements

We would like to thank our colleagues for their assistance in the writing of this article. I would also like to thank my supervisors, Professors Shubei Ma and Hongling Zhao, for repeatedly revising this article and my unit for providing me with the platform. We would also like to thank the United Imaging platform on which the model was trained.I would like to thank American Journal Experts (http://www.aje.cn) for English language editing.

Author contributions

XP, HR, LX, FL, WS, LC and ZC contributed to the study conception and design. XP and HR wrote the first draft of the manuscript. LX, YZ and FL performed the statistical analyses. WS, CL and ZC organized the database. JW and FS performed the imaging analyses and contributed to data collection. SM and HZ edited the manuscript. All the authors contributed to manuscript revision and read and approved the submitted version.All authors reviewed the manuscript.

Funding

This work was supported by the Dalian Central Hospital "peak plan" science and technology project (Grant ID: 2022ZZ215).

Declarations

Ethics approval and consent to participate

This study was approved by the ethics committee of Dalian Municipal Central Hospital (approval number: 2022-039-60). All methods were carried out in accordance with relevant guidelines and regulations. All of the human subjects in this study provided written informed consent for their participation in our research.

Statement

To analyze the relationships among the degree of migraine with RLS, white matter lesions and brain structural volume, 102 migraineurs with RLS were selected. The RLS flow and HIT-6 score were recorded to reflect the degree of headache. The brain structural volumes were calculated with artificial intelligence. The WMLs of migraineurs with RLS were concentrated mainly in the white matter of the lateral ventricular margin and deep white matter. There were significant differences in WML variables among migraineurs with RLS with different HIT-6 grades and MIDAS grades. There was a significant difference in the volume of brain structures, and there was a significant difference among migraineurs with different RLS flows, HIT-6 grades and peripheral cerebrospinal fluid volumes. There was a positive correlation between frontal pole volume and RLS flow. The volume of specific brain structures was negatively correlated with RLS flow but positively correlated with HIT-6 grade. The volume of specific brain structures was negatively correlated with the HIT-6 grade. There was no correlation between WML severity and RLS flow or migraine severity. Volume changes occurred in parts of the brain structures of migraineurs with RLS. Shunt flow and the degree of migraine in migraineurs with RLS were correlated with structural volume changes in some brain regions.

Competing interests

The authors declare no competing interests.

Additional information

Supplementary Information The online version contains supplementary material available at https://doi.org/10.1038/s41598-025-85205-w.

Correspondence and requests for materials should be addressed to H.Z. or S.M.